Thermodynamics of High-Pressure Adsorption of Argon, Nitrogen, and Methane on Microporous Adsorbents

M. M. K. Salem, P. Braeuer, M. v. Szombathely, M. Heuchel, P. Harting, and K. Quitzsch

Institute of Physical and Theoretical Chemistry, Faculty of Chemistry and Mineralogy, University of Leipzig, Linnestrasse 2, 04103 Leipzig, Germany

M. Jaroniec*

Department of Chemistry, Kent State University, Kent, Ohio 44242

Received February 5, 1997. In Final Form: April 13, 1998

Adsorption equilibria of argon, nitrogen, and methane on the 13X molecular sieve and the AS activated carbon were measured at five temperatures over a wide pressure range from 0.1 to 20 MPa using a microbalance. From experimental adsorption isotherms, which are excess functions, the absolute isotherms were calculated using equations of state for a real gas phase. Grand canonical Monte Carlo simulations and density functional theory calculations were carried out in order to explain specific features of the resulting isotherms. Different thermodynamic functions evaluated from the excess and absolute adsorption isotherms were analyzed over a wide pressure range at the average temperature of the range studied.

Introduction

Although physical adsorption of pure gases on different porous solids has been extensively studied over a wide range of temperatures and pressures, the number of works related to adsorption at high pressures is limited. Recent developments in instrumentation for adsorption-based gas separations, such as pressure-swing adsorption,[1,2] stimulate research on the high-pressure adsorption equilibria. Physical adsorption of gases and gas mixtures on microporous materials measured at pressures above 0.1 MPa is of great practical importance not only for industrial separations but also for gas-storage technology.[3−6] During the last 20 years, a growing interest in high-pressure adsorption research has been observed.[7−23]

Until now, the thermodynamic treatments of high-pressure adsorption data were relatively limited.[24−32] This especially concerns an exact discussion of the excess adsorption quantities, which are obtained directly from experiment, and the absolute adsorption quantities, which are easier to understand on the molecular basis. In this paper, the excess, specific, and absolute thermodynamic quantities and their importance for high-pressure adsorption will be discussed.

Excess adsorption isotherms of argon, nitrogen, and methane on the 13X zeolite and AS active carbon measured at five temperatures over a wide pressure range from 0.1 to 20 MPa form the experimental basis of the current work. These adsorption isotherms are typical excess isotherms with a distinct maximum. For both adsorbents, methane isotherms intersected after the maximum. To explain this behavior, grand canonical Monte Carlo simulations were carried out for methane in spherical micropores. In addition, the density functional theory calculations were performed to model methane adsorption in slitlike carbon pores.

* To whom correspondence should be addressed.

(1) Yang, R. T. *Gas Separation by Adsorption Processes*; Butterworths: London, 1987.
(2) Ruthven, D. M.; Shamasuzzaman, F.; Knaebel, K. S. *Pressure Swing Adsorption*; VCH Publishers: New York, 1994.
(3) MacDonald, J. A. F.; Quinn, D. F. *Carbon* **1996**, *34*, 1103.
(4) Malbrunot, P.; Vidal, D.; Vermesse, J. *Appl. Therm. Eng.* **1996**, *16*, 375.
(5) Alcaniz Monge, J.; dela CasaLillo, M. A.; Cazorla Amoros, D.; Linares Solano, A. *Carbon* **1997**, *35*, 291.
(6) MacDonald, J. A. F.; Quinn, D. F. *Fuel* **1998**, *77*, 61.
(7) Menon, P. G. *Chem. Rev.* **1968**, *68*, 277.
(8) Bose, T. K.; Chahine, R.; Marchildon, L.; St-Arnaud, J. M. *Rev. Sci. Instrum.* **1987**, *58*, 2279.
(9) Vidal, D.; Malbrunot, P.; Guengant, L.; Vermesse, J.; Bose, T. K.; Chahine, R. *Rev. Sci. Instrum.* **1990**, *61*, 1314.
(10) Giacobbe, F. W. *Rev. Sci. Instrum.* **1991**, *62*, 2186.
(11) Payne, H. K.; Sturdevant, G. A.; Leland, W. P. *Ind. Eng. Chem. Fundam.* **1968**, *7*, 363.
(12) Osawa, R.; Kusumi, S.; Ogino, Y. *J. Colloid Interface Sci.* **1976**, *56*, 83.
(13) Wakasugi, Y.; Ozawa, S.; Ogino, Y. *J. Colloid Interface Sci.* **1981**, *79*, 399.
(14) Findenegg, G. G. In *Fundamentals of Adsorption*; Engineering Foundation: New York, 1984.
(15) Specovius, J.; Findenegg, G. H. *Ber. Bunsen-Ges. Phys. Chem.* **1978**, *82*, 174; **1980**, *84*, 696.
(16) Benard, P.; Chahine, R. *Langmuir* **1997**, *13*, 808.
(17) Vermesse, J.; Vidal, D.; Malbrunot, P. *Langmuir* **1996**, *12*, 4190.
(18) Pribylov, A. A.; Stoeckli, H. F. *Russ. J. Phys. Chem.* **1968**, *72*, 244.
(19) Pribylov, A. A.; Yakubov, T. S. *Russ. Chem. Bull.* **1996**, *45*, 1078.
(20) Gusev, V.; Fomkin, A. *J. Colloid Interface Sci.* **1994**, *162*, 279.
(21) Aydt, E. M.; Hentschke, R. *Ber. Bunsen-Ges. Phys. Chem.* **1997**, *101*, 79.
(22) Talu, O.; Zhang, S. Y.; Hayhurst, D. T. *J. Phys. Chem.* **1993**, *97*, 12894.
(23) Zhang, S. Y.; Talu, O.; Hayhurst, D. T. *J. Phys. Chem.* **1991**, *95*, 1722.
(24) Gachet, C.; Trambouze, Y. *J. Chim. Phys.* **1990**, *67*, 2072.
(25) Yoshio, H.; Kobayashi, R. *J. Chem. Phys.* **1971**, *54*, 1226.
(26) Yoshio, H.; Kobayashi, R. *Ind. Eng. Chem. Fundam.* **1973**, *12*, 26.
(27) Findenegg, G. G.; Specovius, J. *Ber. Bunsen-Ges. Phys. Chem.* **1980**, *84*, 690.
(28) Blumel, S.; Koster, F.; Findenegg, G. H. *J. Chem. Soc., Faraday Trans. 2* **1982**, *78*, 1753.
(29) Agarwal, R. K.; Schwarz, J. A. *Carbon* **1988**, *26*, 873.
(30) Agarwal, R. K.; Schwarz, J. A. *J. Colloid Interface Sci.* **1989**, *130*, 137.
(31) Agarwal, R. K.; Amankwah, K. A. G.; Schwarz, J. A. *Carbon* **1990**, *28*, 169.
(32) Jagiello, J.; Sanghani, P.; Bandosz, T.; Schwarz, J. *Carbon* **1992**, *30*, 507.

S0743-7463(97)00119-4 CCC: $15.00
Published on Web 05/19/1998

Table 1. Specific Surface Areas $a_{A,sp}$ in m²/g and Specific Pore Volumes $v_{A,sp}$ in cm³/g of the Samples before and after Adsorption

adsorbent	zeolite 13X before adsorption	zeolite 13X after adsorption	carbon AS before adsorption	carbon AS after adsorption
		Specific Surface Area (m²/g)		
BET (∞ layers)	530	560	970	1020
BET (*n* layers)	740 (1.1)	810 (1.1)	1130 (1.9)	1160 (2.0)
		Specific Pore Volumes (cm³/g)		
DR pore volume	0.27	0.30	0.43	0.46
Gurvich rule method	0.30	0.31	0.52	0.54

Table 2. Physicochemical Data for the Adsorbates Used

gas	purity (v/v %)	molecular weight (g/mol)	T_c (K)	p_c (MPa)	ρ_c (g/cm³)	v_c (cm³/mol)	α ($\times 10^{-24}$ cm³)
Ar	99.999	39.948	150.75	4.864	0.531	75.3	1.63
N_2	99.999	28.016	134.15	3.546	0.311	90.1	1.74
CH_4	99.999	16.043	190.65	4.640	0.162	99.0	2.60

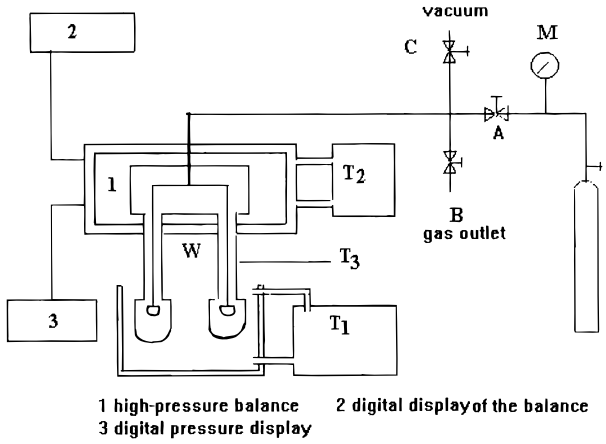

Figure 1. Schematic representation of gravimetric equipment for high-pressure gas adsorption.

Experimental Section

The microporous adsorbents used in the current work were the 13X molecular sieve having the Si/Al ratio 1.18 and the AS activated carbon, which is applied as a respiratory protection carbon. Table 1 shows the specific surface area and the specific pore volume of both adsorbents, respectively. Argon, nitrogen, and methane of a very high purity were purchased from Air Liquide. Table 2 contains important data of the adsorptives used.

Gravimetric Adsorption Equipment. Adsorption measurements were carried out by using a gravimetric apparatus equipped with a Sartorius high-pressure microbalance model S3D−P (see Figure 1). The balance was placed in a housing of stainless steel suitable for measurements up to 20 MPa, which could be evacuated via a vacuum line. The gas can be dosed into the system via valve A. The equilibrium pressure was measured with an accuracy of ±0.1 bar by using a TICON model TIM 84 manometer. The balance system was thermostated to a desired temperature by pumping liquid from an external bath T_2 through the jacket of the housing. The down-tubes of the balance were immersed in liquid thermostat T_1. The temperature was controlled within ±0.1 K.

A known amount of the 13X molecular sieve (∼150 mg), which was activated in helium at the rate 10 K/min up to 673 K and kept at 673 K for 30 min, or active carbon, which was outgassed at 433 K, was placed into the sample pan of the microbalance. After outgassing, the buoyancy correction was determined using high-pressure helium measurements at 303.15 K (helium adsorption was neglected although there are some reports[33−35] about its significance for some adsorption systems) and the system was outgassed again. Adsorption isotherms of argon, nitrogen, and methane were measured in the supercritical pressure range from 0.1 to 20 MPa at five temperatures: 258.15, 273.15, 288.15,; 303.15, and 418.15 K. The equilibrium time for each adsorption point was about 1 h.

Determination of the Buoyancy Correction. The right pan of the microbalance (see Figure 1) contains the adsorbent of mass m_A. The mass of the absolute adsorbed gas should be m_s. The left pan of the balance contains the tare weight of mass m_w. The recorded apparent mass change on the right side caused by the adsorption is

$$\Delta m_T = m_{p,T} - m_{0,T} \tag{1}$$

where $m_{p,T}$ is the mass on the right pan of the balance at the equilibrium pressure p and the adsorption temperature T and $m_{0,T}$ denotes the mass at the same temperature but in a vacuum ($p \rightarrow 0$). The total buoyancy consists of the following individual terms:

$$A_i = M_g \rho_g V_i; \quad i = \text{r, l, A, s, w} \tag{2}$$

where the subscript i refers, respectively, to the right-hand pan (r), the left-hand pan (l), the adsorbent (A), the absolute adsorbed amount (s), and the tare weight (w) on the left side pan. M_g is the molar mass, ρ_g is the density of the adsorptive, and V is the volume of the above-mentioned elements, respectively. The buoyancy of the absolute amount adsorbed A_S cannot be determined, because the volume V_s is unknown. This is the reason for the excess values obtained by gravimetric adsorption measurements. The true mass change (subscript tr) is given by

$$\Delta m_{tr} = \Delta m_T + \Delta A + A_s;$$
$$\Delta A = A_r + A_A - A_l - A_w = M_g \rho_g \Delta V;$$
$$\Delta V = V_r + V_A - V_l - V_w \tag{3}$$

The volume ΔV can be determined by helium measurements under the assumption that helium is not adsorbed at room temperature. Therefore, the following relations exist

$$\Delta A_{He} = M_{He} \rho_{He} \Delta V;$$
$$\Delta A = M_g \rho_g \Delta A_{He} / (M_{He} \rho_{He}); \; \Delta m_{tr} - A_s = \Delta m_T + \Delta A \tag{4}$$

and the adsorption excess amount Γ^σ can be calculated by the following formula:

$$\Gamma^\sigma \equiv n^\sigma / m_A = (n^s - V_s \rho_g)/m_A = (\Delta m_T + \Delta A)/(m_A M_g) \tag{5}$$

where n^σ is the excess amount of the adsorbed gas.

Characterization of Adsorbents. Adsorbents were exposed to a high pressure up to 20 MPa during the adsorption process. Therefore, it was necessary to know if both adsorbents were changed during this process, because all the thermodynamic

(33) Maggs, F. A. P.; Schwabe, P. H.; Williams, J. H. *Nature* **1960**, *186*, 956.
(34) Malbrunot, P.; Vidal, D.; Vermesse, J.; Chahine, R.; Bose, T. K. *Langmuir* **1997**, *13*, 539.
(35) Neimark, A. V.; Ravikovitch, P. I. *Langmuir* **1997**, *13*, 5148.

calculations require that all properties of adsorbents, for example, specific surface area $a_{A,sp}$, specific pore volume $v_{A,sp}$, and others, remain unchanged. For this reason, the adsorbents were analyzed by nitrogen adsorption at 77 K using ASAP 2000M (Micromeritics, Inc., Norcross, GA). Nitrogen adsorption isotherms were needed to determine the specific areas and the specific pore volume of the adsorbent studied by using the following methods: the classical BET equation[36] and its extended form to *n*-layers,[36,37] the t-plot method,[38,39] the Dubinin−Radushkevich equation (DR),[40] the Gruvich rule,[41] and density functional theory (DFT).[42] The resulting data are summarized in Table 1. The specific surface areas 630 and 970 m^2/g and the specific pore volumes 0.27 and 0.43 cm^3/g were obtained for the 13X molecular sieves and AS active carbon, respectively. The pore size distribution functions of the active carbon before and after high-pressure adsorption measurements calculated from nitrogen adsorption isotherms using the DFT method[42] are very similar. Also, the FTIR−Raman spectra recorded for the 13X zeolite before and after high-pressure adsorption do not indicate noticeable changes in the structure of this material. On the basis of these results, one can conclude that the porous structure of the adsorbents studied has not been changed after high-pressure adsorption. Some structural changes during adsorption are possible, but they are reversible.

Adsorption Isotherms

Excess Adsorption Isotherms. Adsorption isotherms of argon, nitrogen, and methane on the 13X molecular sieve and the AS active carbon were calculated from primary experimental quantities using eq 5. They are represented in Figures 2 and 3. All isotherms show maxima, which shift in the direction of high pressures with increasing temperature.

The excess adsorption isotherms of methane on both adsorbents show an additional characteristic feature: they intersect after the maximum. While their temperature dependence until this intersection region is typical as for physisorption, it becomes reserved after this point. A first possible interpretation of this behavior could be related to the change in the adsorbent properties due to high-pressure adsorption, for example, the change in the pore structure, but the pore size distribution functions for the active carbon sample before and after adsorption experiments show no significant difference. Therefore, it can be assumed that high-pressure adsorption did not change the active carbon porous structure. Besides that, the recorded FTIR spectra for the molecular sieve sample studied under the same conditions as the active carbon also do not show significant changes in the adsorbent structure. That means that the reason for the intersection of the adsorption isotherms should be related rather to the properties of adsorptives in either the adsorbed or gas phase. A further discussion of this aspect will be presented later.

All excess adsorption isotherms do not show hysteresis (see Figures 2 and 3). Therefore, it was possible to assume a reversible adsorption process with respect to all adsorptives. Adsorption capacities of the active carbon are greater because its specific pore volume is larger than that of the zeolite. For both adsorbents the adsorption

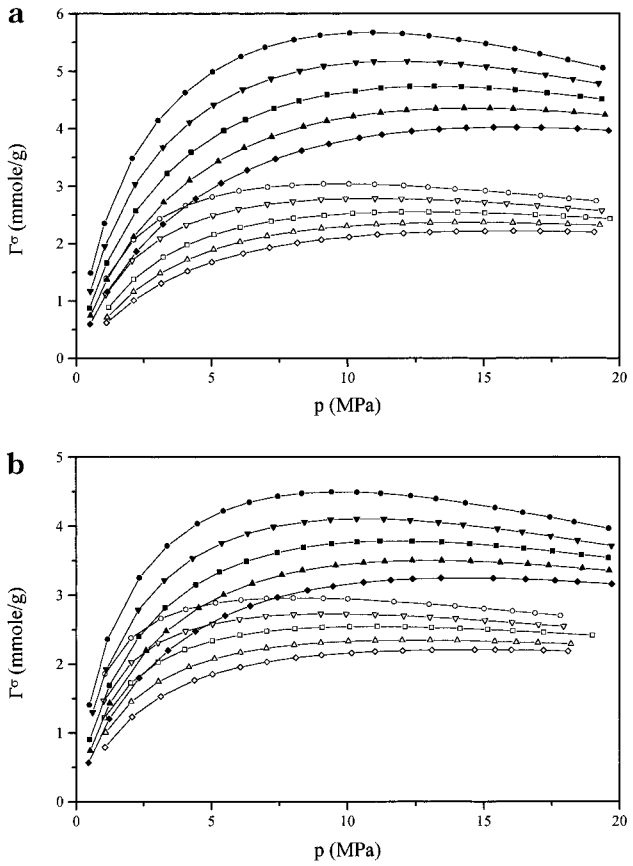

Figure 2. Excess adsorption isotherms of argon (a) and nitrogen (b) on the 13X molecular sieve (open symbols) and AS active carbon (solid symbols) at the temperatures 258.15 K (○, ●), 273.15 K (▽, ▼), 288.15 K (□, ■), 308.15 K (△, ▲), and 318.15 K (◇, ◆).

isotherm of methane is highest in comparison to those for other adsorbates. However, nitrogen adsorption on the zeolite studied is slightly higher than that of argon due probably to interactions of the quadrupole moment of nitrogen molecules with high-energy sites located in the zeolite cavities.[43] It is important to know that argon has a smaller volume, $v_{Ar} = (4\pi/3)(\sigma_{Ar}2)^3 = 0.0217$ nm^3, than nitrogen, $v_{N_2} = (4\pi/3)(\sigma_{N_2}/2)^3 = 0.0276$ nm^3, and therefore the adsorption capacity of argon is greater on active carbon.

Absolute Adsorption Isotherms. Although all experimental quantities for the adsorbed phase, including adsorption isotherms, are the excess ones, many authors consider thermodynamics of excesses as an abstract science. The absolute adsorption is defined as the total amount n^s in the so-called adsorbed phase denoted by the superscript s. To determine this quantity, the total capacity of the adsorbed phase should be known. In the case of flat surfaces, it is very difficult to determine the absolute adsorption because the thickness of the adsorbed phase is unknown. In the case of the adsorbents studied in the current work, it is assumed that the volume of the adsorbed phase is equal to the pore volume V_p. Therefore, knowing the specific pore volume of the adsorbent studied, that is,

$$v_{A,sp} \equiv V_p/m_A \tag{6}$$

it is possible to determine the absolute adsorption isotherm using the definition of the adsorption excess. The excess adsorption n^σ expressed in number of moles is the

(36) Brunauer, S.; Emmett, P. H.; Teller, E. J. *J. Am. Chem. Soc.* **1938**, *60*, 309.
(37) Hill, T. L. *J. Chem. Phys.* **1946**, *14*, 263; **1949**, *17*, 772.
(38) Gregg, S. J.; Sing, K. S. W. *Adsorption, Surface Area and Porosity*; Academic Press: London, New York, 1976.
(39) Lippens, B. C.; de Boer, J. H. *J. Catal.* **1965**, *4*, 319.
(40) Dubinin, M. M.; Zaverina, E. D.; Radushkevich, L. W. *Zh. Fiz. Khim.* **1947**, *21*, 1351 (in Russian).
(41) Gurvich, H. *Zh. Fiz. Khim.* **1915**, *47*, 805 (in Russian).
(42) ASAP 2000 Software, Micromeritics, Inc., Atlanta, GA.
(43) Niwa, M.; Yamazaki, K.; Murakani, Y. *Chem. Lett.* **1989**, *1*, 441.

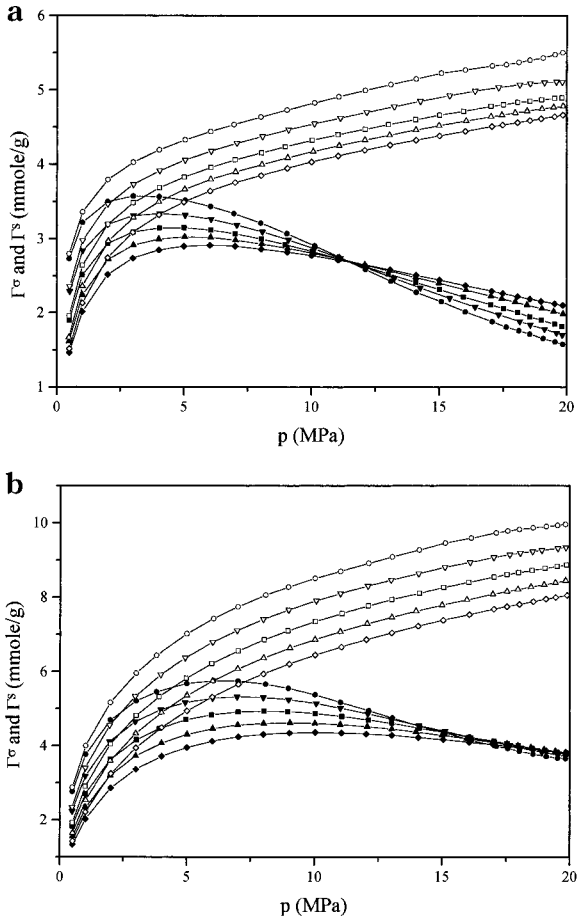

Figure 3. Adsorption excesses (solid symbols) and absolute adsorption isotherms (open symbols) for methane on the 13X molecular sieve (a) and AS active carbon (b) at the temperatures 258.15 K (○, ●), 273.15 K (▽, ▼), 288.15 K (□, ■), 308.15 K (△, ▲), and 318.15 K (◇, ◆).

difference between the absolute adsorption n^s and the number of moles of gas (n^g) in the reference system (all quantities refer to the pore volume V_p):

$$n^\sigma/V_p = n^s/V_p - n^g/V_p \tag{7}$$

The reference system has the same volume V_p as the adsorption system, but the interaction with the solid surface is neglected. Because experimental excess adsorption isotherms are related to the adsorbent mass, the following relationship is also valid:

$$\Gamma^\sigma \equiv n^\sigma/m_A = N^s/m_A - n^g/m_A = \Gamma^s - \Gamma^g \tag{8}$$

The relationship between the two last equations is given by the specific pore volume of the adsorbent (see eq 6). The absolute adsorption Γ^s can be evaluated when Γ^g is known. A procedure for calculation of Γ^g is given below. In this work, the gas phase is considered as a real gas in the entire pressure range studied. It will be shown that all thermodynamic quantities are also functions of the real gas parameters. Therefore, fugacities f of nonadsorbed gases were calculated for all pressures and temperatures studied using a two-parameter corresponding state principle.[44] The relationship between the gas isotherm Γ^g and the fugacity can be obtained from the Lewis expression for the chemical potential of the real gas:

$$\mu^g = \mu^{g\oplus}(T) + RT \ln f \tag{9}$$

where $\mu^{g\oplus}(T)$ is the standard chemical potential, which depends only on the temperature. The corresponding differential change in this chemical potential is

$$dG^g_m \equiv d\mu^g_m = -S^g_m\, dT + V^g_m\, dp \tag{10}$$

where $Y^g_m \equiv Y^g/n^g$ are the molar quantities of the real gas and $Y = S, V$. Two last equations give

$$V^g_m = (\partial\mu^g/\partial p)_T = \frac{RT}{p}(\partial \ln f/\partial \ln p)_T \tag{11}$$

Since

$$V^g_m = V/n^g = V_p/n^g = m_A\nu_{A,sp}/n^g = \nu_{A,sp}/\Gamma^g \tag{12}$$

the gas isotherm can be calculated using the following formula:

$$\Gamma^g = \frac{p\nu_{A,sp}}{RT}\frac{1}{(\partial \ln f/\partial \ln p)_T} \tag{13}$$

In the recent work, fugacity was described by the polynomial

$$f = p(1 + p\sum_{j\geq 1} D_j p^{j-1}) \tag{14}$$

which shows a good convergence, especially at $p \to 0$. Assumption of two or three terms of this polynomial is sufficient for an accurate description of the fugacity. Combination of eqs 13 and 14 gives an analytical expression Γ^g:

$$\Gamma^g = \frac{p\nu_{A,sp}}{RT}\frac{1 + p\Sigma_1}{1 + p(2\Sigma_1 + \Sigma_2)},\ \Sigma_1 = \sum_{j\geq 1} D_j p^{j-1},\ \Sigma_2 = \sum_{j\geq 2} D_j(j-1)p^{j-1} \tag{15}$$

Methane gas isotherms were also calculated by the Benedict−Webb−Rubin (BWR) equation[45] containing 20 coefficients.[46] The deviations between the values calculated using the BWR equation and the two-parameter corresponding state principle were negligible. The gas isotherms for methane calculated according to eq 15 are presented in Figure 4, whereas the corresponding absolute isotherms are shown in Figure 3. The gas isotherms have no special features, and their dependence on temperature is as expected for physical adsorption. The isotherms for other adsorptives show similar behavior.

Monte Carlo Simulations and Density Functional Theory Calculations of Adsorption Isotherms. To

(44) Sievers, U.; Schultz, S. *The Thermodynamic Properties of Methane*; VDI-Forschungsheft No. 622; Verein Deutscher Ingenieure: Duesseldorf, 1984.

(45) Belovoshko, A.; Saxena, S. K. *Geochim. Cosmochim. Acta* **1991**, *55*, 3191.

(46) Benedict, M.; Webb, G. B.; Rubin, L. C. *J. Chem. Phys.* **1940**, *8*, 334.

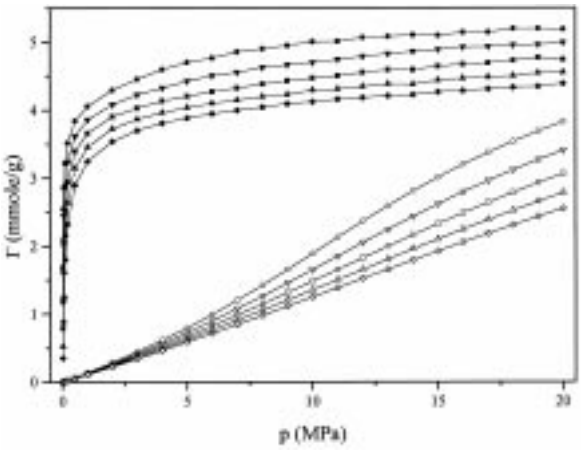

Figure 4. Absolute adsorption isotherms of methane on the 13X molecular sieve (solid symbols) calculated by using the GCMC method and gas isotherms for methane (open symbols) obtained by the Benedict−Webb−Rubin equation at the temperatures 258.15 K (○, ●), 273.15 K (▽, ▼), 288.15 K (□, ■), 308.15 K (△, ▲) and 318.15 K (◇, ◆).

understand the behavior of experimental excess adsorption isotherms, suitable grand canonical Monte Carlo (GCMC) calculations were carried out for adsorption of methane in spherical micropores. It was not the aim of the current work to focus on sophisticated simulations of adsorption equilibria but rather to recognize a general adsorption behavior and to explain the intersection of the excess adsorption isotherms and its thermodynamic consequences. Therefore, a simple model was assumed for the interaction energy between adsorbed molecules and zeolite, in which the zeolite cavity was considered as an energetically homogeneous sphere with a radius of 0.65 nm consisting of oxygen atoms spread on the spherical surface. The specific pore volume of the zeolite was assumed to be 0.30 cm^3/g.[38] The interaction energy between adsorbed methane molecules was described by an exp-6-potential with the parameters $\epsilon/k_B = 140.94$ K and $\sigma = 0.3717$ nm, where k_B is the Boltzmann's constant.[45] However, the interaction between methane and an oxygen atom on the wall of the zeolite cavity was described by the Lennard−Jones potential, the parameters of which were evaluated from the parameters of methane and oxygen using the Lorentz−Berthelot mixing rules. The interaction between oxygen atoms was specified by the following parameters: $\epsilon/k_B = 106.7$ K and $\sigma = 0.3467$ nm.[45] The total interaction energy between adsorptive and adsorbent was calculated by integration over the volume of the spherical pore. To adjust the total interaction energy to the real one, the density was fitted to give the isosteric heat of adsorption of 20.1 kJ/mol for methane on the 13X zeolite at small coverages.[38] The GCMC adsorption isotherms simulated are the absolute isotherms. The excess adsorption isotherms were obtained from them by means of eq 8 and using the gas isotherms Γ^g (see Figure 4) for methane calculated via the Benedict−Webb−Rubin equation with 20 coefficients.[46,47] A comparison of the gas isotherms with the absolute adsorption isotherms shows that the temperature dependence of the former isotherms is greater. That is the reason for the intersection of the excess adsorption isotherms $\Gamma^\sigma = \Gamma^s - \Gamma^g$. The experimental excess adsorption isotherms of methane on zeolite and those obtained by the Monte Carlo method are compared in Figure 5. Although the model used for the

(47) Bender, E. *Cryogenics* **1975**, *15*, 667.

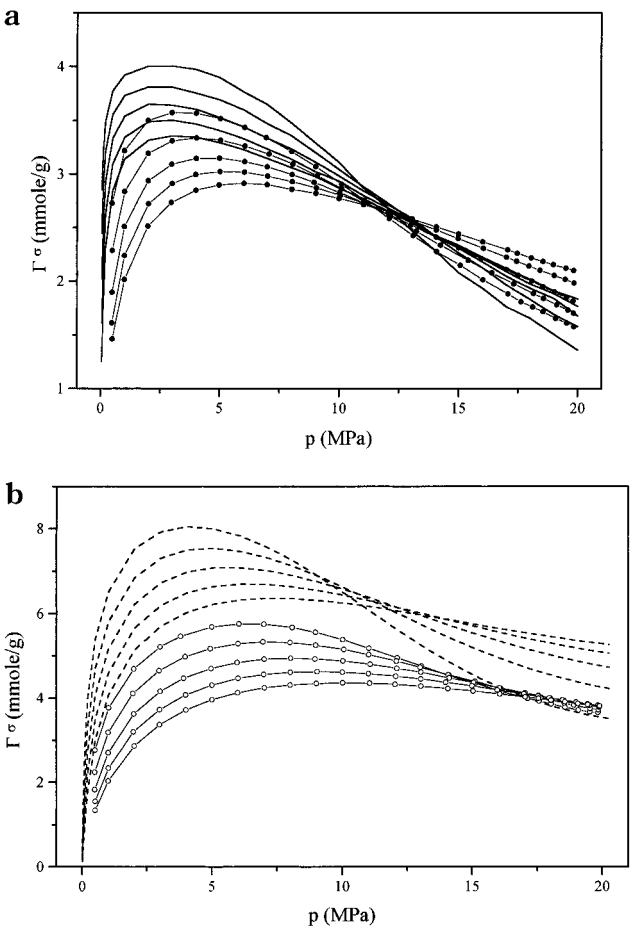

Figure 5. (a) Excess adsorption isotherms for methane on the 13X zeolite obtained experimentally (−●−) and calculated by using the GCMC simulations (−) and (b) adsorption excess isotherms for methane on active carbon obtained experimentally (−○−) and calculated by using the DFT method (- - -).

GCMC simulations was rather crude, the simulation data show the same features as the experimental isotherms.

Furthermore, density functional theory (DFT) calculations were performed to evaluate the excess adsorption of methane in slitlike carbon micropores using similar molecular parameters to those in the case of the GCMC method. The parameters used to model the interaction between carbon atoms were $\epsilon/k_B = 28.0$ K and $\sigma = 0.34$ nm.[48,49] The results presented in Figure 5 in comparison to the experimental isotherms show qualitatively the same behavior as those in the case of simulated data. A poor quantitative agreement between the experimental and theoretical results is due mainly to the fact that the active carbon studied has a wide pore size distribution function consisting of micropores and mesopores, whereas the computer simulations were carried out only for one pore width, $12\sigma_{methane}$.

Description of Isotherms by Different Polynomials and Other Equations. For thermodynamic analysis of adsorption isotherms by means of a computer program, it is convenient to represent those isotherms by analytical functions instead of tabulated data. Therefore, three different polynomials were used to describe the excess

(48) Steele, W. A. *The Interaction of Gases with Solid Surfaces*; Pergamon Press: Oxford, 1974.

(49) Brauer, P.; Poosch, H.-R.; v. Szombathely, M.; Heuchel, M.; Jaroniec, M. Proceedings of the 4th International Conference on Fundamentals of Adsorption. *Stud. Surf. Sci. Catal.* **1993**, *80*, 67.

and absolute isotherms:

$$\Gamma^\sigma = \sum_{j\geq 1} E_j p^{j-1}; \quad \Gamma^s = \sum_{j\geq 1} A_j p^j \tag{16}$$

$$\Gamma^\sigma = p\ \exp(\sum_{j\geq 1} E_j p^{j-1}); \Gamma^s = p\ \exp(\sum_{j\geq 1} A_j p^{j-1}) \tag{17}$$

$$\Gamma^\sigma = \exp\left[\sum_{j\geq 1} E_j \left(\ln \frac{p}{p_m}\right)^j\right]; \Gamma^s = \exp\left[\sum_{j\geq 1} A_j \left(\ln \frac{p}{p_m}\right)^j\right]; \quad p \leq p_m \tag{18}$$

The third formula, which has a thermodynamic background, was already used by one of the authors[50] to describe adsorption on energetically heterogeneous surfaces. Not only do the two last formulas allow us to obtain an excellent representation but their smoothing properties are also very good. For all polynomials listed, about 8−12 coefficients are necessary for a satisfactory description of experimental adsorption isotherms (Supporting Information available for coefficients of eq 17).

Many attempts were made to describe the absolute adsorption isotherms Γ^s with the help of different adsorption equations, which were derived for specific adsorption models, for example, Langmuir, Fowler−Guggenheim, Kiselev, Hill−de Boer, and others.[51,52] Since all of these equations have only a few adjustable parameters, it was impossible to obtain a satisfactory representation of all absolute adsorption isotherms studied. A similar opinion was expressed elsewhere.[24] However, in refs 9 and 10 the excess adsorption isotherms Γ^σ of methane on zeolites of type X and Y containing different cationic forms were approximated by the temperature-dependent exponential virial expression with only a few parameters, but these data were measured only at the pressure range below 7 MPa, in which the excess isotherms do not have maxima. As mentioned above, the application of eqs 16−18 (which have mathematical forms of virial expansions) to describe the absolute isotherms up to the pressure of 20 MPa requires also several parameters.

Fundamental Thermodynamic Relations

Concept of Thermodynamic Excess Quantities. The thermodynamic considerations presented below are essentially based on an elegant thermodynamic treatment of interfacial problems formulated by Lopatkin and Vernov.[53,54] Since experimental adsorption quantities are the excess ones, basic thermodynamic equations should be formulated for these quantities, especially when the gravimetric method is applied. Any extensive excess quantity is defined as follows:

$$Y^\sigma \equiv Y^{het} - Y^g - Y^A; \quad dY^\sigma = dY^{het} - dY^g - dY^A \tag{19}$$

where the superscript het stands for the entire heterogeneous adsorption system. The reference system consists of the gas phase g without contact with the solid surface and the solid phase A under vacuum or in contact with a nonadsorbing inert gas, for example, helium (see Figure 6). If accompanying processes (i.e., absorption of gases or dissolution of the solid in the gas phase) can be excluded, then an extensive excess quantity Y^σ defined by eq 19 can be rewritten as follows:

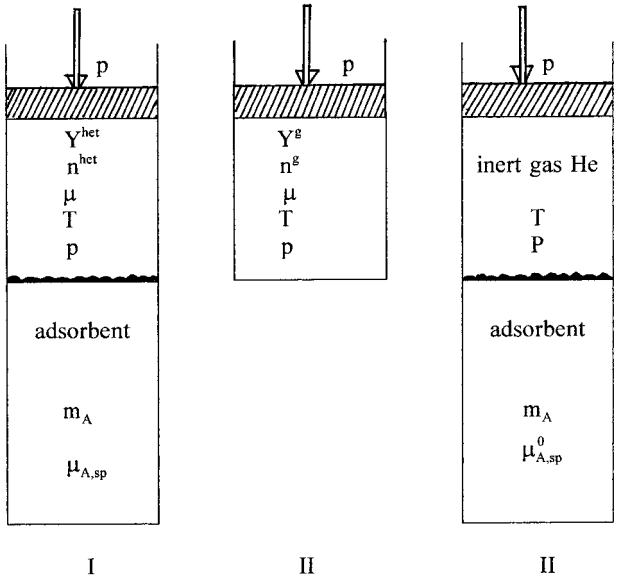

Figure 6. Schematic illustration of the thermodynamic approach to the excess adsorption quantities: (I) real heterogeneous adsorption system; (II) reference system.

$$Y^\sigma = Y^{het} - Y^A = Y^{het} - n^g Y^g_m - m_A y_{A,sp} \tag{20}$$

where Y^g_m is the molar quantity of the gas phase and $y_{A,sp}$ is the specific quantity of the solid related to the adsorbent mass m_A. The fundamental thermodynamic relationship between excess quantities is

$$dU^\sigma = T\ dS^\sigma + \mu\ dn^\sigma + \Phi\ dm_A; \quad U^\sigma = TS^\sigma + \mu n^\sigma + \Phi m_A \tag{21}$$

where μ is the chemical potential of the gas in the adsorbed and nonadsorbed state and Φ is the symbol for the difference between the specific chemical potential of the adsorbent in contact with the adsorbed gas and the potential without this contact, that is, in a vacuum or in contact with a nonadsorbing inert gas:

$$\Phi \equiv \mu_{A,sp} - \mu^\circ_{A,sp} \tag{22}$$

Therefore, Φ can be regarded as a measure of the change in the chemical potential of the adsorbent due to adsorption. Because the volume of a heterogeneous adsorption system v^{het} is equal to the volume of the reference system $v^g + v^A$, the excess volume $V^\sigma \equiv 0$ and eq 21 does not contain a term for the volume work (although in refs 53 and 54 the excess volume V^σ was assumed to be different than zero, its value was very small in comparison to the gas-phase volume V^g). For that reason, the following are valid: $H^\sigma \equiv U^\sigma$; $G^\sigma \equiv A^\sigma$. The Gibbs function and the Gibbs−Duhem equation obtained from eq 21 are

$$dG^\sigma = -S^\sigma\ dT + \mu\ dn^\sigma + \Phi\ dm_A; \quad G^\sigma = \mu n^\sigma + \Phi m_A \tag{23}$$

$$-S^\sigma\ dT - n^\sigma\ d\mu - m_A\ d\Phi = 0; \quad d\mu = S^\sigma_{m,int}\ dT - (1/\Gamma^\sigma)\ d\Phi \tag{24}$$

(50) Jaroniec, M. *Surf. Sci.* **1975**, *50*, 553.
(51) Harting, P.; Weingart, K.; Schwarz, G. *Isotopenpraxis* **1990**, *26*, 512.
(52) Braeuer, P.; Jaroniec, M.; Salem, M.; v. Szombathely, M.; Heuchel, M.; Harting, P. *Proceedings of the Second International Symposium, Effects of Surface Heterogeneity in Adsorption and Catalysis on Solids*, Zakopane, Poland and Levoca, Slovakia, September, 1995; M.C.S. University: Lublin, Poland, 1995.
(53) Lopatkin, A. A. *Theoretical Foundations of Physical Adsorption*; Izdatelstvo Moskovskogo Universiteta: Moscow, 1983 (in Russian).
(54) Vernov, A. v.; Lopatkin, A. A. *Zh. Fiz. Khim.* **1979**, *53*, 2333, 3161; **1980**, *54*, 2327; **1981**, *55*, 438 (in Russian).

where the integral molar adsorption excess quantities are defined by $Y^{\sigma}_{m,int} \equiv Y^{\sigma}/n^{\sigma}$ and the adsorption excess Γ^{σ} is defined by eq 8. According to eq 24, the chemical potential of the adsorbed molecules is a function of T and Φ. To obtain not only integral molar, but also differential molar quantities from thermodynamic relations, it is convenient to express the chemical potential also as a function of temperature and adsorption excess:

$$d\mu = (\partial\mu/\partial T)_{\Gamma^{\sigma},m_A}\, dT + (\partial\mu/\partial\Gamma^{\sigma})_T\, d\Gamma^{\sigma};$$
$$(\partial\mu/\partial T)_{\Gamma^{\sigma},m_A} = -(\partial S^{\sigma}/\partial n^{\sigma})_{T,m_A} \equiv -S^{\sigma}_{m,diff} \quad (25)$$

The last term in eq 25 was obtained by applying the Schwarz theorem to eq 23. A combination of the condition for the adsorption equilibrium $\mu \equiv \mu^g$ $d\mu \equiv d\mu^g$ at T = constant and p = constant with the expression for the change in the chemical potential of the gas phase, $d\mu^g = -S^g_m\, dT + V^g_m\, dp$, leads to fundamental equations for the excess adsorption:

$$-(S^{\sigma}_{m,int} - S^g_m)\, dT - V^g_m\, dp - (1/\Gamma^{\sigma})\, d\Phi = 0 \quad (26)$$

$$-(S^{\sigma}_{m,diff} - S^g_m)\, dT - V^g_m\, dp - (\partial\mu/\partial\Gamma^{\sigma})_T\, d\Gamma^{\sigma} = 0 \quad (27)$$

which can be directly applied to the existing experimental conditions. The differential form of the Gibbs adsorption equation at constant temperature can be obtained from eq 26:

$$(\partial\Phi/\partial p)_T = -V^g_m\Gamma^{\sigma} \quad (28)$$

Integration of this equation leads to its integral form $\Phi = -\int_0^p V^g_m\Gamma^{\sigma}\, dp$ which expressed in terms of the compressibility factor $Z = pV^g_m/RT$ is

$$\Phi = -RT\int_0^p Z\Gamma^{\sigma}\, d\ln p \quad (29)$$

Z can be calculated using the gas fugacity calculated by means of the expression $Z = (\partial \ln f/\partial \ln p)_T$ or using the fugacity coefficients $\varphi \equiv f/p$ obtained on the basis of the following equation: $Z = 1 + (\partial \ln \varphi/\partial \ln p)_T$. As can be seen from eq 29, the assumption that the nonadsorbed phase is a real gas is sufficient to calculate Φ and all other thermodynamic quantities, which can be evaluated from it. At low pressures, $Z \cong 1$ and eq 29 can be divided into a Henry region term and a second term related to equilibrium pressures outside this range:

$$\Phi = -RT\Gamma^{\sigma}_{Henry} - RT\int_{p_{Henry}}^p Z\Gamma^{\sigma}\, d\ln p \quad (30)$$

where p_{Henry} and Γ^{σ}_{Henry} are the values at the end of the Henry region. If the specific surface area $a_{A,sp} \equiv A/m_A$ of the adsorbent is known (e.g., evaluated by nitrogen adsorption), the quantity Φ can be replaced by the surface pressure $\pi = \gamma - \gamma°$, which is defined as the difference between the surface tension of the solid covered with adsorbed molecules γ and the surface tension of that solid in a vacuum or in contact with an inert nonadsorbed gas $\gamma°$. Then the relation $\Phi\, dm_A = -\pi\, dA$ combined with eq 30 yields

$$\pi = -RT\hat{\Gamma}^{\sigma}_{Henry} - RT\int_{p_{Henry}}^p Z\hat{\Gamma}^{\sigma}\, d\ln p \quad (31)$$

where the adsorption excess related to the solid surface is defined by $\hat{\Gamma}^{\sigma} \equiv n^{\sigma}/A$.

On the basis of eqs 30 and 31, one can calculate the thermodynamic integral molar excess adsorption quantities using eq 26 at a constant pressure. The change in an integral molar excess quantity is defined as follows:

$$\Delta Y^{\sigma}_{m,int} \equiv Y^{\sigma}_{m,int} - Y^g_m \quad (32)$$

then the integral molar excess entropy change $\Delta S^{\sigma}_{m,int}$ caused by adsorption (see eq 26) is given by

$$\Delta S^{\sigma}_{m,int} \equiv S^{\sigma}_{m,int} - S^g_m = -(\partial\Phi/\partial T)_p/\Gamma^{\sigma} \quad (33)$$

The change in the integral molar excess Gibbs' energy $\Delta G^{\sigma}_{m,int}$ can be obtained from eq 23 and is connected with the Gibbs−Helmholtz equation in the following way:

$$\Delta G^{\sigma}_{m,int} \equiv G^{\sigma}_{m,int} - G^g_m \equiv \Delta H^{\sigma}_{m,int} - T\Delta S^{\sigma}_{m,int} = H^{\sigma}_{m,int} - H^g_m - T(S^{\sigma}_{m,int} - S^g_m) = \Phi/\Gamma^{\sigma} \quad (34)$$

On the basis of eqs 33 and 34, one can calculate the change in the integral molar excess enthalpy $\Delta H^{\sigma}_{m,int}$ or the integral molar excess heat of adsorption Q^{σ}_{int} as follows:

$$\Delta H^{\sigma}_{m,int} \equiv H^{\sigma}_{m,int} - H^g_m = [\partial(\Phi/T)/\partial(1/T)]_p/\Gamma^{\sigma} = -Q^{\sigma}_{int} \quad (35)$$

On the other hand, eq 27 allows the evaluation of the different molar excess adsorption quantities. From eq 23 and the equilibrium condition for adsorption, one can get

$$(\partial G^{\sigma}/\partial n^{\sigma})_{T,m_A} \equiv G^{\sigma}_{m,diff} = \mu;$$
$$\Delta G^{\sigma}_{m,diff} \equiv G^{\sigma}_{m,diff} - G^g_m = \mu - \mu^g = 0 \quad (36)$$

Therefore, relationships for the change in the differential molar excess entropy and enthalpy or the differential molar excess heat of adsorption (the so-called isosteric heat of adsorption) can be obtained as follows:

$$\Delta H^{\sigma}_{m,diff} \equiv H^{\sigma}_{m,diff} - H^g_m = T\Delta S^{\sigma}_{m,diff} \equiv T(S^{\sigma}_{m,diff} - S^g_m) = RZ[\partial \ln p/\partial(1/T)]_{\Gamma^{\sigma}} = -Q^{\sigma}_{st} \quad (37)$$

Because the high-pressure adsorption isotherms possess maxima, the adsorption isosters $[\partial \ln p/\partial(1/T)]_{\Gamma^{\sigma}}$ are ambiguous. But with the help of the following simple thermodynamic relation $(\partial p/\partial T)_{\Gamma^{\sigma}}(\partial\Gamma^{\sigma}/\partial p)_T(\partial T/\partial\Gamma^{\sigma})_p = -1$ the isoteric differential quotient can be expressed as the ratio of two differential quotients:

$$[\partial \ln p/\partial(1/T)]_{\Gamma^{\sigma}} = -\frac{[\partial \ln \Gamma^{\sigma}/\partial(1/T)]_p}{(\partial \ln \Gamma^{\sigma}/\partial \ln p)_T} \quad (38)$$

The specific heat of adsorption Δh^{σ}_{sp} related to the mass of the adsorbent can be directly measured by calorimetry. A simple setup of the calorimetric equipment is shown in Figure 7. Prior to making adsorption measurements the adsorbent of mass m_A is placed in the cuvette of the calorimeter under vacuum at temperature T. The total volume of the adsorption system V^{het} consists of the gas volume measured with helium V_{He} and the volume V^0_A of the unperturbed solid. The last volume can be determined from $V^0_A = V^{het} - V_{He}$. The adsorption system is separated from the dosage system by valve 1. If the pressure of the

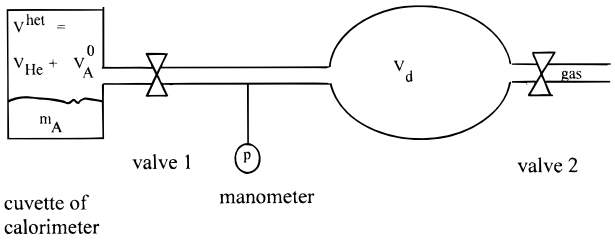

Figure 7. Simple schematic representation of an adsorption calorimeter.

dosed volume is p_d, the amount of gas contained in that volume is

$$n_d = \frac{p_d V_d}{RT}\frac{1}{Z(p_d)}$$

where $Z(p_d)$ is the compressibility factor at the pressure p_d. In order to start gas adsorption, valve 1 should be opened, and after establishing the adsorption equilibrium at temperature T and pressure p, the amount of gas contained in the volume $V_{He} + V_d$ can be obtained from the real gas equation

$$n^g = \frac{p(V_{He} + V_d)}{RT}\frac{1}{Z(p)}$$

The difference between these two gas amounts is the adsorption excess

$$n^\sigma = n_d - n^g = \frac{p_d V_d}{RT}\frac{1}{Z(p_d)} - \frac{p(V_{He} + V_d)}{RT}\frac{1}{Z(p)} \qquad (39)$$

where $Z(p_d)$ is the compressibility factor at the pressure p_d. The enthalpy of the total system before adsorption H_{before} consists of the enthalpy of the adsorbent under vacuum conditions H_0^A and the enthalpy of the gas in the dosed volume H_d^g, that is,

$$H_{before} = H_0^A + H_d^g = m_A h_{A,sp}^0 + n_d[H_m^g(p_d)]$$

where $h_{A,sp}^0$ is the specific enthalpy of the adsorbent in vacuum and $H_m^g(p_d)$ is the molar enthalpy of the gas in the dosage system at pressure p_d. The enthalpy of the total system after adsorption consists of the enthalpy of the unperturbed adsorbent, the enthalpy of the gas under adsorption equilibrium conditions H^g, and the excess enthalpy H^σ, that is,

$$H_{after} = H_0^A + H^g + H^\sigma = m_A h_{A,sp}^0 + n^g[H_m^g(p)] + H^\sigma$$

where $H^g{}_m(p)$ is the molar enthalpy of the gas at the equilibrium pressure. All changes caused by adsorption, for example, the perturbation of the adsorbent, are contained in the excess enthalpy H^σ. Then the specific excess enthalpy change, which is related to the adsorption process, is given as follows:

$$\Delta h_{sp}^\sigma \equiv \frac{\Delta H^\sigma}{m_A} \equiv \frac{H_{after} - H_{before}}{m_A} = \frac{H^\sigma}{m_A} + \frac{n^g}{m_A}H_m^g(p) - \frac{n_d}{m_A}H_m^g(p_d) \qquad (40)$$

Now, it is possible to compare this quantity with the integral molar excess enthalpy defined by $H^\sigma{}_{m,int} \equiv H^\sigma/n^\sigma$ and obtained from the adsorption isotherm data using eq 35:

$$\Delta h_{sp}^\sigma = \Gamma^\sigma H_{m,int}^\sigma + \frac{n^g}{m_A}H_m^g(p) - \frac{n_d}{m_A}H_m^g(p_d) \qquad (41)$$

This comparison can be done if the molar enthalpy of the gas phase H_m^g is known. In principle, it is possible to calculate the pressure dependence of H_m^g using the thermodynamic equation of state:

$$(\partial H_m^g/\partial p)_T = V_m^g - T(\partial V_m^g/\partial T)_p$$

which expressed in terms of the compressibility factor Z has the following form:

$$(\partial H_m^g/\partial p)_T = -\frac{RT^2}{p}(\partial Z/\partial T)_p$$

However, there is another possibility for evaluating these enthalpy differences. If the gas volume of the adsorption system V_{He} is small in comparison to the volume of the dosage system V_d, then the pressure difference $\Delta p = p_d - p$ due to the expansion of the gas from the dosage system to the adsorption system by opening valve 1 is small and $H_m^g(p_d) \approx H_m^g(p) \equiv H_m^g$. Then, eq 41 becomes

$$\Delta h_{sp}^\sigma = \Gamma^\sigma(H_{m,int}^\sigma - H_m^g) = \Gamma^\sigma \Delta H_{m,int}^\sigma \qquad (42)$$

In this way it is possible to compare the enthalpy values calculated from the excess adsorption isotherms with those obtained calorimetrically. It should be noted that, in the case of adsorption isotherm measurements, the establishment of the equilibrium state is usually a process of a few hours or days, whereas the calorimetric measurement is an irreversible short time process, which usually requires a few minutes.

The specific entropy and Gibbs function changes can be obtained from calorimetric data, if their temperature dependence is known, by using the following equations:

$$\Delta h_{sp}^\sigma = \left[\frac{\partial(\Delta g_{sp}^\sigma/T)}{\partial(1/T)}\right]_p; \quad \Delta g_{sp}^\sigma = \Delta h_{sp}^\sigma - T\Delta s_{sp}^\sigma \qquad (43)$$

Concept of Thermodynamic Absolute Quantities. A thermodynamic consideration of absolute adsorption quantities requires the assumption of a layer at the solid surface, that is, the absorbed phase. This phase includes a specified region of the gas phase adjacent to the solid surface separated from the remaining part of the gas phase by a dividing plane, so-called the Gibbs dividing surface. In general, this approach has a subjective moment, because the thickness of the adsorbed layer or the volume of the adsorbed phase must be known. While thermodynamic excess quantities change continuously from the solid surface to the bulk phase, the absolute quantities show a jump transition between the adsorbed phase and the gas phase. The absolute thermodynamic values for a given adsorption system are average quantities, and therefore they are constant within the adsorbed phase.

It was shown in refs 53 and 54 that the same thermodynamic approach can be applied for the absolute adsorption quantities if the reference system is chosen as

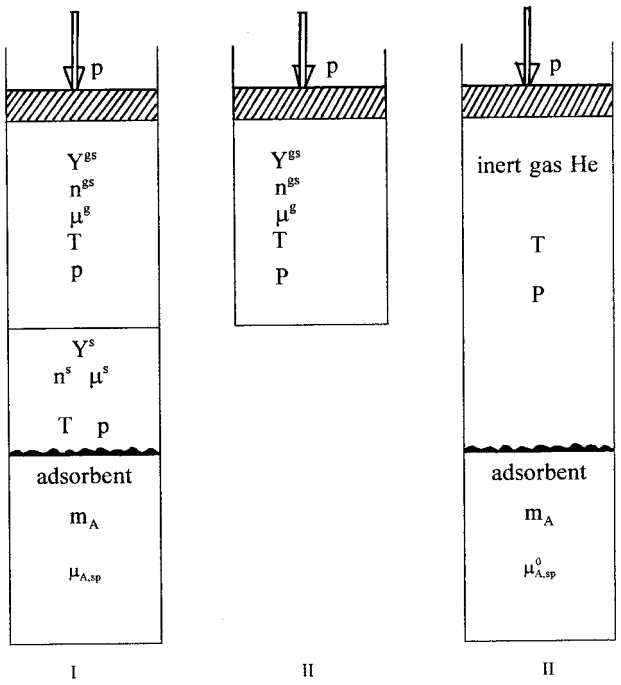

Figure 8. Schematic illustration of the thermodynamic approach to the absolute adsorption quantities: (I) heterogeneous adsorption system; (II) reference system.

illustrated in Figure 8. Then, instead of eqs 19 and 20, the absolute extensive quantities are defined as follows:

$$Y^s \equiv Y^{het} - Y^{gs} - Y^A = Y^{het} - n^{gs}Y^g_m - m_A y_{A,sp}; \quad dY^s = dY^{het} - dY^{gs} - dY^A \quad (44)$$

where the superscripts s and gs stand for the adsorbed phase and for the gas phase of the reference system as shown in Figure 8, respectively. By eliminating Y^{het} in eqs 20 and 44, one can derive a general relation between the extensive absolute and excess gas adsorption quantities:

$$Y^s = Y^\sigma + Y^g - Y^{gs} = Y^\sigma + (n^g - n^{gs})Y^g_m \quad (45)$$

Finally, instead of eqs 23 and 24, eqs 46 and 47 are obtained:

$$dG^s = -S^s\,dT + V^s\,dp + \mu^s\,dn^s + \Phi\,dm_A; \quad G^s = \mu^s n^s + \Phi m_A \quad (46)$$

$$-S^s\,dT + V^s\,dp - n^s\,d\mu^s - m_A\,d\Phi = 0; \quad d\mu^s = -S^s_{m,int}\,dT + V_{m,int}\,dp - (1/\Gamma^s)\,d\Phi \quad (47)$$

where μ^s is the chemical potential of the gas in the adsorbed phase and the integral molar absolute adsorption quantities are defined by $Y^s_{m,int} \equiv Y^s/n^s$. It is easy to show that $\Phi^s \equiv \Phi^\sigma \equiv \Phi$, because, in the terminology of absolute quantities, Φ is also defined by eq 22 and therefore it is independent of the specific description of a heterogeneous adsorption system. Equation 47 represents the surface-phase chemical potential μ^s as a function of T, p, and Φ. As can be seen from eq 46, the chemical potential μ^s can be represented also as a function of T, p, and n^s/m_A, that is,

$$\mu^s = \mu^s(T,p,n^s,m_A) = \mu^s(T,p,\Gamma^s) \quad (48)$$

$$d\mu^s = (\partial\mu^s/\partial T)_{p,\Gamma^s}\,dT + (\partial\mu^s/\partial p)_{T,\Gamma^s}\,dp + (\partial\mu^s/\partial\Gamma^s)_{T,p}\,d\Gamma^s \quad (49)$$

$$(\partial\mu^s/\partial T)_{p,\Gamma^s} = -(\partial S^s/\partial n^s)_{T,p,m_A} \equiv -S^s_{m,diff}; \quad (\partial\mu^s/\partial p)_{T,\Gamma^s} = (\partial V^s/\partial n^s)_{T,p,m_A} \equiv V^s_{m,diff} \quad (50)$$

Applying the condition for the thermodynamic equilibrium between the adsorbed and gas phases

$$(\mu^s \equiv \mu^g; \quad d\mu^s \equiv d\mu^g \text{ at } T = \text{constant and } p = \text{constant})$$

and the expression for the change in the chemical potential in the gas phase, one can get two fundamental equations for the absolute gas adsorption, which are analogues of eqs 26 and 27:

$$-(S^s_{m,int} - S^g_m)\,dT + (V^s_{m,int} - V^g_m)\,dp - (1/\Gamma^s)\,d\Phi = 0 \quad (51)$$

$$-(S^s_{m,diff} - S^g_m)\,dT + (V^s_{m,diff} - V^g_m)\,dp - (\partial\mu^s/\partial\Gamma^s)_{T,p}\,d\Gamma^s = 0 \quad (52)$$

In a very similar way, as in the case of the excess quantities, one can obtain, on the basis of eqs 51 and 52, the integral and differential molar absolute adsorption quantities, which are defined as follows:

$$\Delta Y^s_{m,int} \equiv Y^s_{m,int} - Y^g_m; \quad \Delta Y^s_{m,diff} \equiv Y^s_{m,diff} - Y^g_m \quad (53)$$

The equations given below replace eqs 33−37.

$$\Delta S^s_{m,int} \equiv S^s_{m,int} - S^g_m = -(\partial\Phi/\partial T)_p/\Gamma^s \quad (54)$$

$$\Delta G^s_{m,int} \equiv G^s_{m,int} - G^g_m \equiv \Delta H^s_{m,int} - T\Delta S^s_{m,int} = H^s_{m,int} - H^g_m - T(S^s_{m,int} - S^g_m) = \Phi/\Gamma^s \quad (55)$$

$$\Delta H_{m,int} \equiv H^s_{m,int} - H^g_m = [\partial(\Phi/T)/\partial(1/T)]_p/\Gamma^s = -Q^s_{int} \quad (56)$$

$$(\partial G^s/\partial n^s)_{T,p,m_A} \equiv G^s_{m,diff} = \mu^s; \quad \Delta G^s_{m,diff} \equiv G^s_{m,diff} - G^g_m = \mu^s - \mu^g = 0 \quad (57)$$

$$\Delta H^s_{m,diff} \equiv H^s_{m,diff} - H^g_m = T\Delta S^s_{m,diff} \equiv T(S^s_{m,diff} - S^g_m) = RZ[\partial \ln p/\partial(1/T)]_{\Gamma^s} = -Q^s_{st} \quad (58)$$

Application of Derived Thermodynamic Relations to Experimental Adsorption Isotherms

As was shown above, different thermodynamic quantities (see Table 3) can be calculated from the excess and absolute adsorption isotherms. These thermodynamic quantities will be discussed with respect to their ability to provide information about the adsorption process and the molecular properties of the adsorbed phase.

Extrapolation of Adsorption Isotherms to the Low-Pressure Region and Its Influence on Thermodynamic Quantities. The commercially available

Table 3. Different Thermodynamic Quantities Obtained from Excess and Absolute Adsorption Isotherms Using Thermodynamic Relationships

	excess quantities	absolute quantities
integral molar quantities	$\Delta Y^{\sigma}_{m,int} = Y^{s}_{m,int} - Y^{g}_{m}$	$\Delta Y^{s}_{m,int} = Y^{s}_{m,int} - Y^{g}_{m}$
differential molar quantities	$\Delta Y^{\sigma}_{m,diff} = Y^{s}_{m,diff} - Y^{g}_{m}$	$\Delta Y_{m,diff} = Y^{s}_{m,diff} - Y^{g}_{m}$
specific quantities	$\Delta y^{\sigma}_{sp} = \Gamma^{\sigma}\Delta Y^{s}_{m,int}$	$\Delta y^{s}_{sp} = \Gamma^{s}\Delta Y^{s}_{m,int}$

equipment for high-pressure adsorption does not allow us to measure isotherms at pressures below approximately 1 bar. This fact considerably complicates the thermodynamic analysis of adsorption data. While the differential molar quantities do not provide information about the behavior of the system below the first experimental pressure point, the integral molar and specific quantities possess a systematical error of unknown magnitude. Therefore, an extrapolation of the measured isotherm to zero pressure ($p = 0$) is necessary; that is, its Henry's region must be found. We have noticed that the application of the polynomial eq 17 for mathematical description of the excess and absolute adsorption isotherms is very effective. Also, it was demonstrated by using the low pressure, the GCMC simulations, and the DFT adsorption data.

Two functions, that is, the specific Gibbs energy Φ and the specific excess enthalpy Δh^{σ}_{sp}, were chosen to illustrate consequences of the extrapolation of data points to zero pressure. The integrand of eq 30, which gives at $p \rightarrow 0$ the Henry's constant K_H, is shown in Figure 9a. If one assumes that the Henry's region starts at the first experimental point, which is necessary when extrapolation is not used, then the lower curves are obtained. In the case of extrapolation of the data by the polynomial eq 17, the upper values of the Henry's constant are obtained. Table 4 presents the Henry's constants calculated from the adsorption data with and without extrapolation to zero pressure.

The influence of the isotherm extrapolation on Φ and on the specific excess enthalpy is shown in Figure 9b. A systematical error arising from the assumption that the Henry's region begins already at the first measured isotherm point is of unknown magnitude and has a greater effect on the thermodynamic quantities, which were calculated from Φ, than on the quantity Φ itself. In Figure 10 the quantity Φ is shown as a function of the pressure (Figure 10a) or the adsorption excess (Figure 10b) for methane adsorbed on zeolite at different temperatures. An intriguing behavior of Φ in Figure 10b is explainable by the fact that all excess adsorption isotherms Γ^{σ} show maxima. In Figure 10c, the specific Gibbs energies for argon, nitrogen, and methane on the zeolite 13X and active carbon are compared at the average temperature 288.15 K. If one interprets the negative value of Φ as the adsorption affinity, then it is noticeable that Φ is greater for all adsorptives in the case of active carbon which contains micropores and mesopores. However, for the molecular sieve 13X, which possesses acid groups in the form of the $Na^{+}(AlO_4)$ species, the adsorption affinity increases in the order from argon and nitrogen to methane in accordance with their polarizabilities, as shown in Table 2. The higher values obtained for nitrogen than for argon can be explained by additional interactions between the quadrupole moment of nitrogen and the above-mentioned charged surface groups of the zeolite. In the case of active carbon which contains chemical groups of smaller charge, the values for argon are only slightly higher than those for nitrogen.

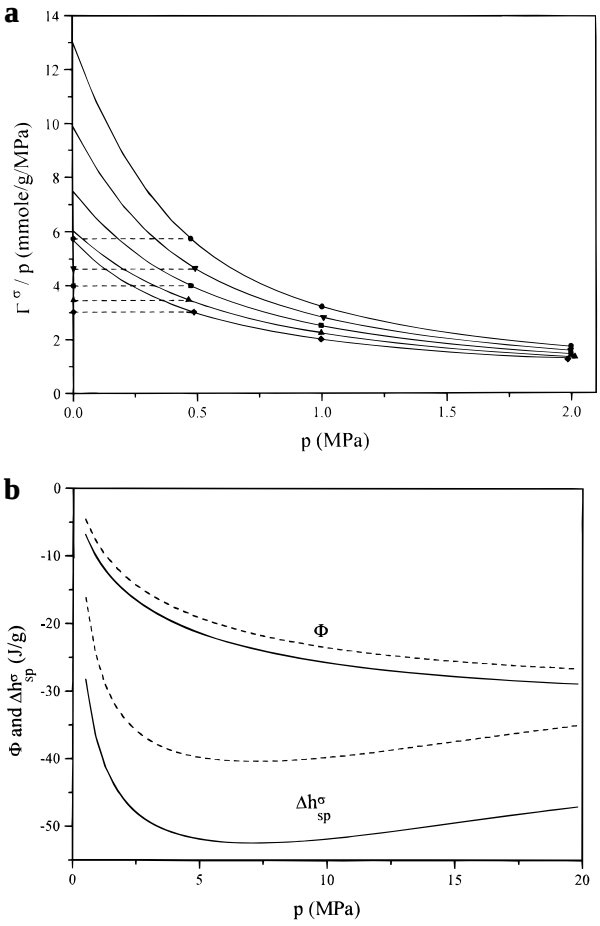

Figure 9. Influence of the extrapolation of the Henry range $p \rightarrow 0$ on the thermodynamic functions of methane adsorbed on zeolite at the average temperature 288.15 K: (a) integrand of eq 30; (b) specific Gibbs energy and specific excess enthalpy. Solid lines were obtained by using the extrapolated Henry's constant, and dashed lines were obtained without this extrapolation.

Table 4. Values of the Logarithm of the Henry's Constant for the Methane/Zeolite System Calculated from the First Isotherm Point ($K_H = \Gamma^{\sigma}_1/p_1$) and by Extrapolation of the Polynomial Eq 17 to $p \rightarrow 0$ ($K_H = e^{E_1} = e^{A_1}$)

temp (K)	calc without extrapolation $\ln K_H = \ln(\Gamma_1/p_1)$	calc by extrapolation using the polynomial eq 17 $\ln K_H = C1$
258.15	1.747	2.555
273.15	1.539	2.278
288.15	1.387	1.999
303.15	1.244	1.807
318.15	1.107	1.708

Calculation of Thermodynamic Differential Molar Excess Quantities. The differential molar excess enthalpies and entropies were calculated using eqs 37 and 38. The differential quotient in the denominator of eq 38 was determined by using the polynomial eq 17. To evaluate the differential quotient $(\partial \ln \Gamma^{\sigma}/\partial(1/T)_p)$ in the numerator, the cubic spline functions were applied to describe the function $\ln \Gamma^{\sigma} = f(1/T)$. The isosteric excess adsorption heat Q^{σ}_{st} calculated in this way is presented in Figure 11 as a function of the equilibrium pressure p. Because the denominator of eq 38 is equal to zero at the maximum of the isotherms $\Gamma^{\sigma}_T(p)$, the isosteric excess heat as well as the differential molar entropy changes show an asymptote, respectively, which is nonrealistic. After the asymptote, the heat has negative values. This

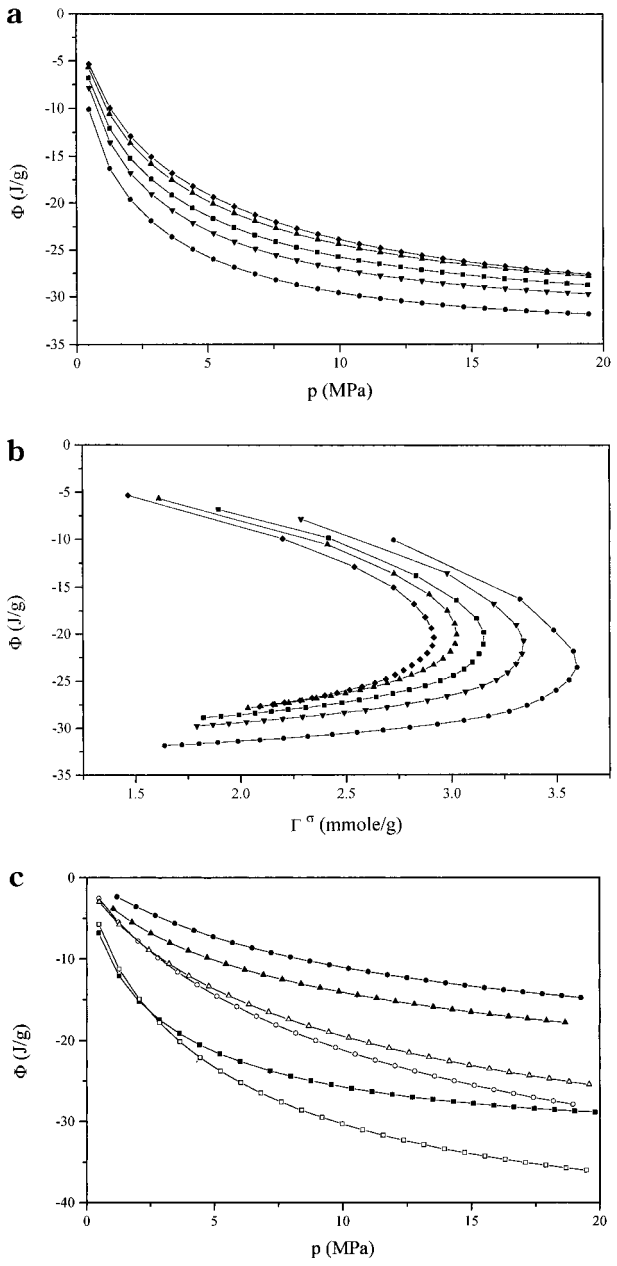

Figure 10. Specific Gibbs energy Φ for adsorption of methane on the 13X molecular sieve plotted as a function of the equilibrium pressure (a) and the excess adsorbed amount (b) at the temperatures 258.15 K (●), 273.15 K (▼), 288.15 K (■), 308.15 K (▲), and 318.15 K (◆) and (c) the Gibbs energy Φ of argon (○, ●), nitrogen (△, ▲), and methane (□, ■) adsorbed on zeolite (solid symbols) and active carbon (open symbols) at the average temperature 288.15 K.

could be understood as an endothermic behavior, which is not typical for physisorption. Chemisorption is excluded for the applied adsorptives. On the other hand, at very high pressures, the isosteric heat becomes again positive due to the inverse temperature dependence of the isotherms after the intersection point. On the basis of these facts, one can conclude that it is necessary to reexamine the concept of the isosteric heat of adsorption in the case of high-pressure adsorption. The heat from Figure 11 cannot be regarded as a quantity of real physical meaning but only as a mathematical value obtained from adsorption isosteres.

Calculation of Thermodynamic Integral Molar Excess Quantities. The integral molar adsorption excess quantities can be calculated by means of eqs 33, 34, and

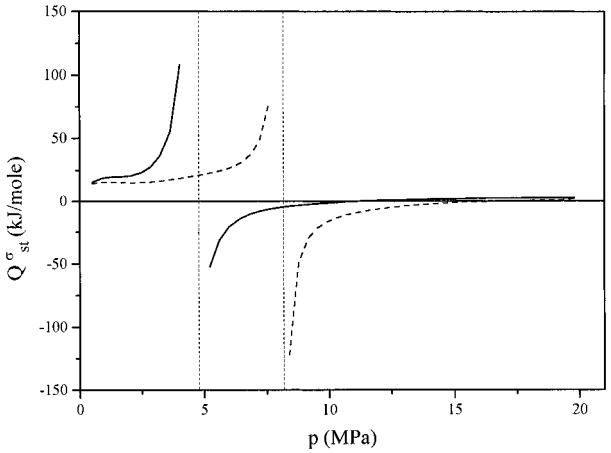

Figure 11. Isosteric excess heat plotted as a function of the equilibrium pressure for adsorption of methane on the 13X molecular sieve (solid line) and active carbon (dashed line) at the average temperature 288.15 K.

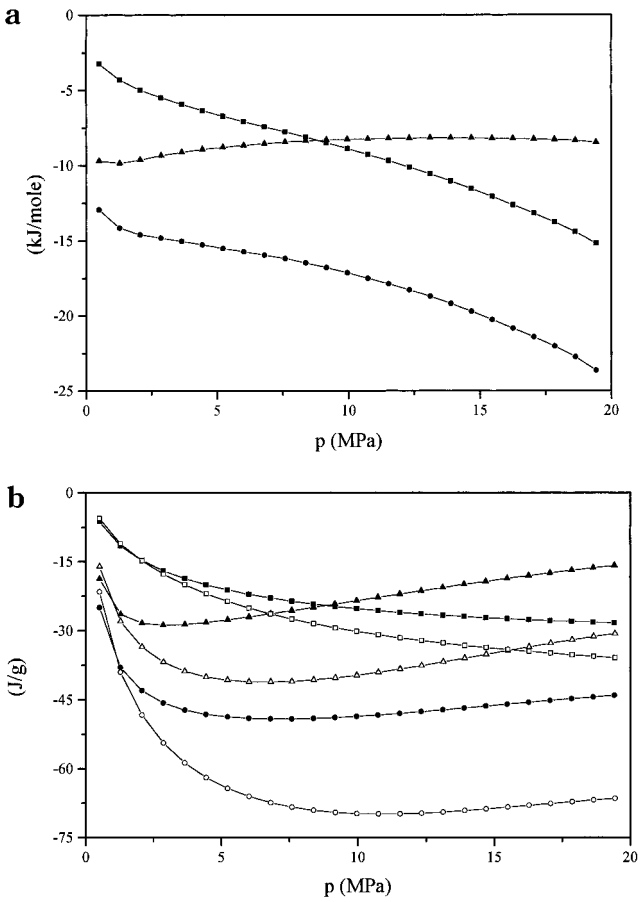

Figure 12. (a) Integral molar excess quantities $\Delta G^{\sigma}_{m,int}$ (■), $\Delta H^{\sigma}_{m,int}$ (●), and $T\Delta S^{\sigma}_{m,int}$ (▲) for methane adsorbed on the 13X molecular sieve and (b) the specific quantities Δg^{σ}_{sp} (□, ■), Δh^{σ}_{sp} (○, ●), and $T\Delta s^{\sigma}_{sp}$ (△, ▲) for methane adsorbed on the 13X molecular sieve (solid symbols) and active carbon (open symbols), plotted as functions of the equilibrium pressure at the average temperature 288.15 K.

35. They are shown in Figure 12a for adsorption of methane on both adsorbents. Also, these quantities have unrealistic behavior at $p \rightarrow \infty$.

Determination of Thermodynamic Specific Excess Quantities. In contrast to the integral molar excess adsorption quantities $\Delta Y^{\sigma}_{m,int}$, the specific excess quantities Δy^{σ}_{sp} can be measured directly, that is, calori-

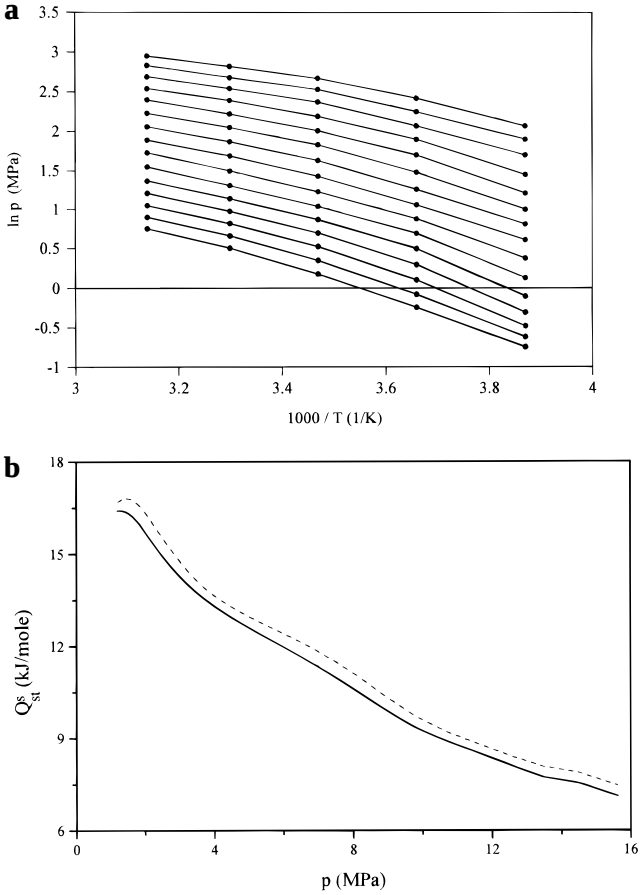

Figure 13. Absolute adsorption isosters (a) and the corresponding absolute isosteric heats of adsorption (b) plotted as functions of the equilibrium pressure for methane/zeolite 13X at the average temperature 288.15 K using the cubic smoothing spline functions (solid line) and linear regression method (dashed line) to describe the temperature dependence of the isosters.

metrically. Their values calculated from adsorption excess isotherms by means of eqs 42 and 43 are shown in Figure 12b for methane adsorbed on zeolite 13X and on active carbon AS. All values are negative in the whole pressure region, which in the case of the adsorption affinity $\Delta g^{\sigma}_{sp} \equiv \Phi$ indicates the spontaneity of the adsorption process and in the case of the specific enthalpy change suggests its exothermic character. Finally, the negative values of the specific entropy changes can be explained by gradual ordering of the molecules in the pores of both adsorbents in contrast to the molecules in the gas phase. The specific excess quantities are zero at $p = 0$ and achieve constant values at $p \rightarrow \infty$.

Calculation of Absolute Differential Molar Adsorption Quantities. Absolute adsorption isosters and the absolute isosteric heat of adsorption (obtained via eq 58) plotted as functions of the equilibrium pressure are shown in Figure 13a and b for the methane/zeolite 13X system. The curvature of the isosters is due to the real gas properties in the gas and adsorbed phases. The differential quotient in eq 58 was calculated in two different ways. According to the first way, the isosters were approximated by the linear function

$$\ln p = A + B\frac{1}{T}; \quad Q^s_{st} = -RZB \tag{59}$$

where the parameters were evaluated by the linear regression analysis neglecting the curvature of the isosteres. According to the second way, the isosters were described by the cubic smoothing spline functions, taking into account their curvature. As can be seen from Figure 13b, the curvature of the isosters has only a little influence on the main behavior of the isosteric heat. Using the polynomial eq 17 to describe the absolute adsorption isotherms, one can calculate the Henry's constant for each isotherm and obtain its temperature dependence and use these data to evaluate the isosteric heats of adsorption at zero coverage. It appeared that the resulting values of the isosteric heat of adsorption were too small. Therefore, the following polynomial was used to describe the isosteric heat of adsorption as a function of the equilibrium pressure

$$Q^s_{st} = \exp\left(\sum_{j\geq 1} C_j p^{j-1}\right); \quad \lim_{p\rightarrow 0} Q^s_{st} = \exp(C_1) \tag{60}$$

in order to obtain its extrapolated values at $p = 0$ (see Table 5), which are analogous to the values reported elsewhere. An exact comparison of the calculated heats with those reported in the literature (see refs 14, 24, 31, and 55− 60) obtained experimentally as well as theoretically in terms of statistical thermodynamics is difficult because adsorption conditions such as temperature, the type of adsorbent, its pretreatment and handling before adsorption, the method of evaluating the heat of adsorption at zero coverage, and so on are different. Figure 14 shows the isosteric heats of adsorption (including the extrapolated curves—dashed lines) calculated from the isosters described by the cubic smoothing splines expressed as functions of the equilibrium pressure and absolute adsorbed amount at the average temperature. The behavior of all curves, which are decreasing functions, is similar. They should be considered as an interplay between the interaction energy of molecules with the pore wall and the interaction energy between them. In the initial stage of adsorption, molecules are located on the pore wall and their lateral interaction energy is lower than the effect of the surface heterogeneity. Therefore, the heat curves decrease. When the pore walls are occupied by adsorbed molecules, more adsorbing molecules fill the center of pores. Therefore, the heat curves show a further decrease because the adsorbate−adsorbent interaction energy inside pores is smaller than the adsorbate−adsorbate interaction energy. It should be noted that from a thermodynamical viewpoint it is impossible to separate the influence of the adsorbate−adsorbent and adsorbate−adsorbate interactions from the overall heat of adsorption. But in the case of the GCMC simulations this separation is possible. Although the model used in simulations was

Table 5. Absolute Isosteric Heats of Adsorption at $p \rightarrow 0$ or $\Gamma^s = 0$ Calculated Using the Polynomial Eq 60

adsorbent	gas	Q^s_{st} in kJ/mol at $p \rightarrow 0$ and $T = 288.15$ K
zeolite 13X	argon	10.94
	nitrogen	13.91
	methane	17.53
active carbon AS	argon	11.80
	nitrogen	11.95
	methane	14.35

(55) Loughlin, K. F.; Hasanain, M. A.; Abdul-Rehman, H. B. *Ind. Eng. Chem. Res.* **1990**, *29*, 9, 1535.
(56) Sams, J. R.; Constabaris, G.; Halsey, G. D. *J. Phys. Chem.* **1960**, *64*, 1689.
(57) Constabaris, G.; Sams. J. R.; Halsey, G. D. *J. Phys. Chem.* **1961**, *65*, 367.
(58) Braüer, P.; Kiselev, A. V.; Lopatkin, A. A.; Shpigil, S. *Dokl. Akad. Nauk SSSR* **1965**, *161*, 853.
(59) Barrer, R. M.; Stuart, W. S. *Proc. R. Soc.* **1959**, *A249*, 464.
(60) Barrer, R. M.; Sutherland, J. M. *Proc. R. Soc.* **1956**, *A237*, 1211.

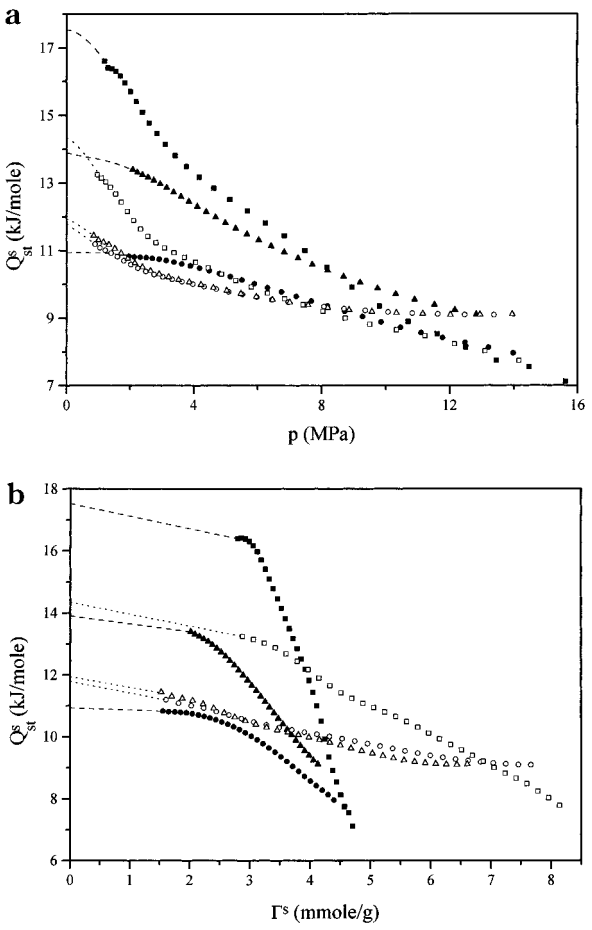

Figure 14. Absolute isosteric heats of adsorption of argon (○, ●), nitrogen (△, ▲), and methane (□, ■) on the molecular sieve (solid symbols) and active carbon (open symbols) plotted as functions of the equilibrium (a) and absolute adsorption amount (b) at the average temperature 288.15 K. Points denote the values obtained from experimental isosters, and dashed lines denote the values obtained with the help of the polynomial eq 60.

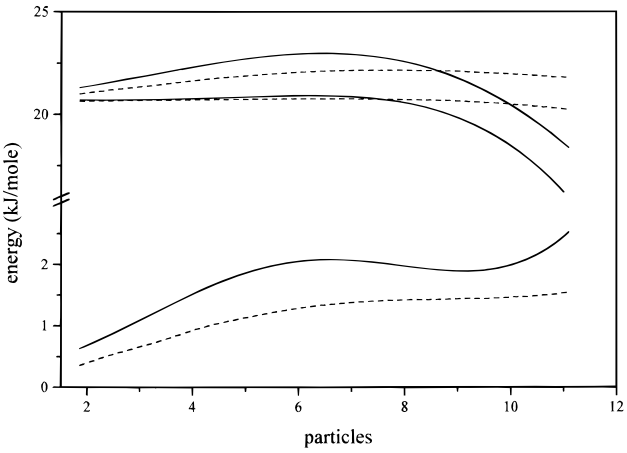

Figure 15. GCMC differential (solid lines) and integral (dashed lines) molar energies plotted as a function of the number of methane molecules in the 13X zeolite cavity. Curves on the top represent the total interaction energy and the interaction energy with the wall; curves on the bottom are the lateral interaction energies.

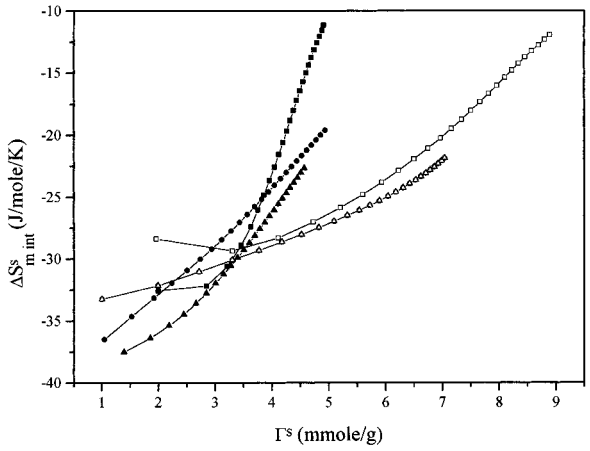

Figure 16. Absolute integral molar entropy change for argon (○, ●), nitrogen (△, ▲), and methane (□, ■) adsorbed on the 13X molecular sieve (solid symbols) and AS active carbon (open symbols) plotted as a function of the absolute adsorbed amount at the average temperature 288.15 K. The curves for argon and nitrogen on active carbon coincide.

simple because of the assumption that the zeolite cavities are energetically homogeneous, the simulation results were useful for explaining the main behavior of molecules in the real system. In Figure 15, the differential and integral molar energies, of molecules in the zeolite cavity are divided into two parts: the interaction energy of molecules with the pore walls and the lateral interaction between adsorbed molecules. As can be seen from the differential energies, about seven molecules can be adsorbed on the wall with nearly constant adsorption energy. However, the total energy is increasing because the lateral energy is increasing too. Beginning with the eighth molecule, both the interaction energy with the pore wall and the total energy are decreasing because the adsorption energy in the center of the cavity is smaller than the increase in the lateral interaction energy.

In the real case, the wall of the zeolite cavity has a strong energetical heterogeneity. Therefore, the heat curves show only a decreasing behavior. If one compares the heat curves for all adsorptives on the different adsorbents, then it is obvious that the energetical heterogeneity of the zeolite is pronounced due to the above-mentioned acidic $Na^-(AlO_4)^-$ groups. In the case of active carbon, the curves for argon and nitrogen are in principle not different, which is evident from the viewpoint of nearly equal polarizabilities. In the case of molecular sieves, the interaction between the acidic groups and the quadrupole moment of nitrogen leads to a higher heat curve. The heat curves of argon on both adsorbents show no remarkable differences, whereas, in the case of methane, they differ considerably. That can be explained by a higher induction interaction energy between methane and the acidic group because this energy is proportional to the polarizability of the adsorbed molecule (see Table 2). Comparing the heat curves plotted as a function of the equilibrium pressure with those plotted as a function of the adsorbed amount, one can notice that adsorption starts at comparable pressures but the starting coverages are different (see Figure 14a). At the same starting pressure of 2 MPa, the starting coverages in the zeolite cavities are proportional to the polarizabilities of adsorptives.

Calculation of Absolute Integral Molar Adsorption Quantities. Integral molar absolute adsorption quantities $\Delta Y^s_{m,int}$ can be calculated from the temperature dependence of the adsorption affinity Φ using eqs 54−56. Note that the entropy change is of special interest because its value can be used to evaluate the entropy of molecules in the adsorbed phase if the entropy of the gas phase is known. As shown in Figure 16 the absolute integral molar entropy changes are negative in the whole pressure range.

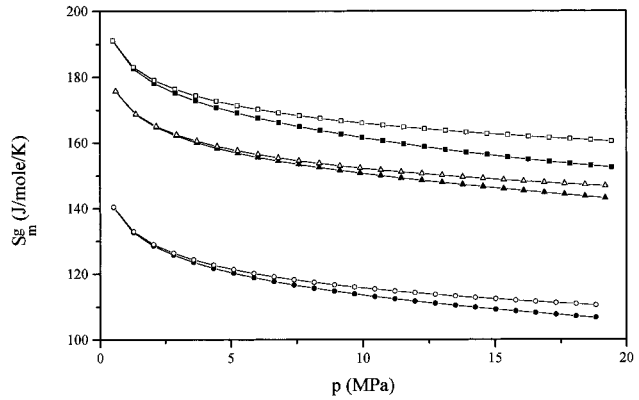

Figure 17. Total entropies (solid symbols) and their ideal parts (open symbols) of gaseous argon (○, ●), nitrogen (△, ▲) and methane (□, ■) as a function of the pressure at the temperature 288.15 K.

That is an evidence for higher entropy of the gas phase, in which molecules have a lower degree of ordering than those inside pores.

Evaluation of Adsorption Entropies for the Gas-Phase Using Statistical Thermodynamic Relations. Absolute molar entropies of the adsobed phase can be estimated from the entropy changes in Figure 16, if the entropy of the gas phase is known

$$S^s_m = \Delta S^s_{m,int} + S^g_m = R \ln W^s \qquad (61)$$

where W^s is the thermodynamic probability of molecules in the adsorbed phase, which can be considered as a measure of order or disorder for molecules inside pores. The entropy of the gas phase can be divided into an ideal part and real parts:

$$S^g_m = S^g_{m,ideal} + S^g_{m,real};$$
$$S^g_{m,real} = -R \ln \varphi - RT(\partial \ln f/\partial T)_p \qquad (62)$$

where the real part can be calculated from the fugacity f and the fugacity coefficients φ, which can be obtained from experimental data using the polynomial eq 14. The differential quotient in eq 62 was obtained with the help of cubic spline functions. The ideal part of the gas entropy was calculated by using statistical thermodynamics relations. The entropies of the gas phase calculated in this way are represented in Figure 17 as a function of the equilibrium pressure at the average temperature $T =$ 288.15 K. The real part gave negative values of the entropy, which are less than 1% of the total entropy. The gas entropy increases from argon to methane, which is connected with the increase in the number of rotational degrees of freedom (2 for nitrogen and 3 for methane). In the case of nitrogen, vibrations do not contribute to the entropy, whereas for methane the low-frequency vibrations give only a negligible amount of 0.345 J/(mol K). The entropies of molecules in pores are shown in Figure 18. The order of changes is the same as that for the gas-phase entropies and is explainable in terms of different degrees of freedom for various adsorptives. Comparing adsorption entropies with those for the gas phase, one can notice two

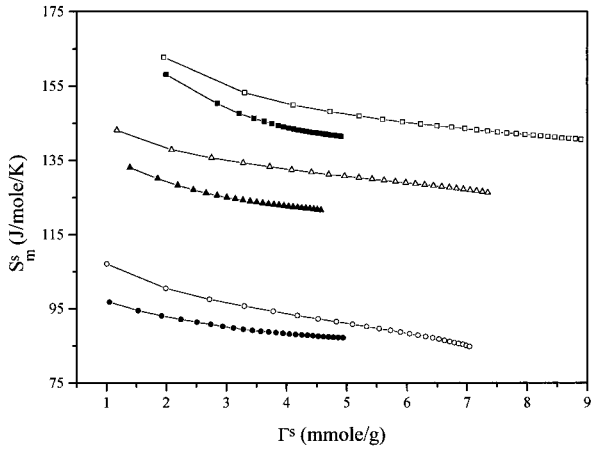

Figure 18. Absolute molar entropies of the adsorbed phase for argon (○, ●), nitrogen (△, ▲), and methane (□, ■) on the molecular sieve (solid symbols) and active carbon (open symbols) at 288.15 K plotted as functions of the absolute adsorbed amount.

aspects. Firstly, the entropies in the adsorbed phase are smaller than those in the gas phase because the degree of ordering is greater. Secondly, the entropy of the adsorbed phase decreases much more slowly with increasing pressure than that in the gas phase. That means that the ordering of molecules inside pores increases much more slowly than that in the gas phase probably due to steric effects.

Conclusions

For a consistent thermodynamic interpretation of high-pressure excess adsorption data it was necessary to consider the specific adsorption quantities. However, they depend strongly on the initial values of adsorption, that is, the Henry's region. If this region is unknown, then the integral molar and specific adsorption quantities are estimated with a systematic error of unknown magnitude. Therefore, in the case of high-pressure adsorption, the low-pressure region must be measured too. However, the current commercial adsorption instruments do not have this option.

A molecular interpretation of high-pressure adsorption data can be done only by using the absolute isosteric and differential molar adsorption quantities. In the case of microporous adsorbents, their evaluation is relatively easy. However, it becomes very difficult in the case of high-pressure adsorption on macroporous and nonporous solids.

Acknowledgment. This work was supported by the Deutsche Forschungsgemeinschaft (The College of Graduate Research on "Physical Chemistry of Interfaces" at the University of Leipzig) and by the Fond der Chemischen Industrie.

Supporting Information Available: Coefficients of the exponential (eq 17), which gives an excellent representation of the excess adsorption isotherms measured for argon, nitrogen, and methane on the 13X molecular sieve and AS active carbon at five different coefficients (11 pages). Ordering information is given on any current masthead page.

LA970119U